PROCEEDINGS OF SCIENCE

Scattering Observables from Few-Body Densities and Application in Light Nuclei

Alexander Long,[a,*] **Harald Griesshammer,**[a] **Andreas Nogga**[b] **and Xiang-Xiang Sun**[b]

[a] *The George Washington University*
Washington DC USA
[b] *Name of Andreas' institution here*
E-mail: alexlong@gwu.edu, hgrie@gwu.edu, a.nogga@fz-juelich.de, x.sun@fz-juelich.de

The dynamics of scattering on light nuclei is well understood, but calculation is numerically difficult using standard methods. Fortunately using recent developments, the relevant quantities can be factored into a product of the n-body transition densities and the interaction kernel of a chosen probe. These transition densities depend only on the target, and not the probe; they are calculated once and stored. The kernels depend on only the probe and not the target. The calculation of the transition densities becomes numerically difficult for $n \geq 4$, but we discuss a solution through use of a renormalization group transformation. This technique allows for extending the density transition method to ^{4}He and ^{6}Li. Throughout this work Compton scattering is used as test bed but extension to pion-photoproduction is discussed as well.

The 11th International Workshop on Chiral Dynamics (CD2024)
26-30 August 2024
Ruhr University Bochum, Germany

*Speaker

 ISSN 1824-8039 . Published by SISSA Medialab.

1. Introduction

This can be 10 pages. Anything is red is a question or something that needs to be fixed.

I am a little unclear on how much discussion of effective field theories, and general intro information is needed here.

The transition density method was pioneered by Griesshammer *et al.*[1]. An incoming probe striking an A body nucleus may interact with $1, 2...A$ nucleons. The n nucleons it interacts with we call *active* and $A - n$ it does not we call *spectators*. The mathematical description of these two parts are completely separate; the active nucleons contribute to the kernel and spectator nucleons contribute to the density. The complete separation of these two parts means if one has access to a different kernels and b different nucleus descriptions, then ab different results can be produced. Figure 1 provides an example for the case $A = 3$.

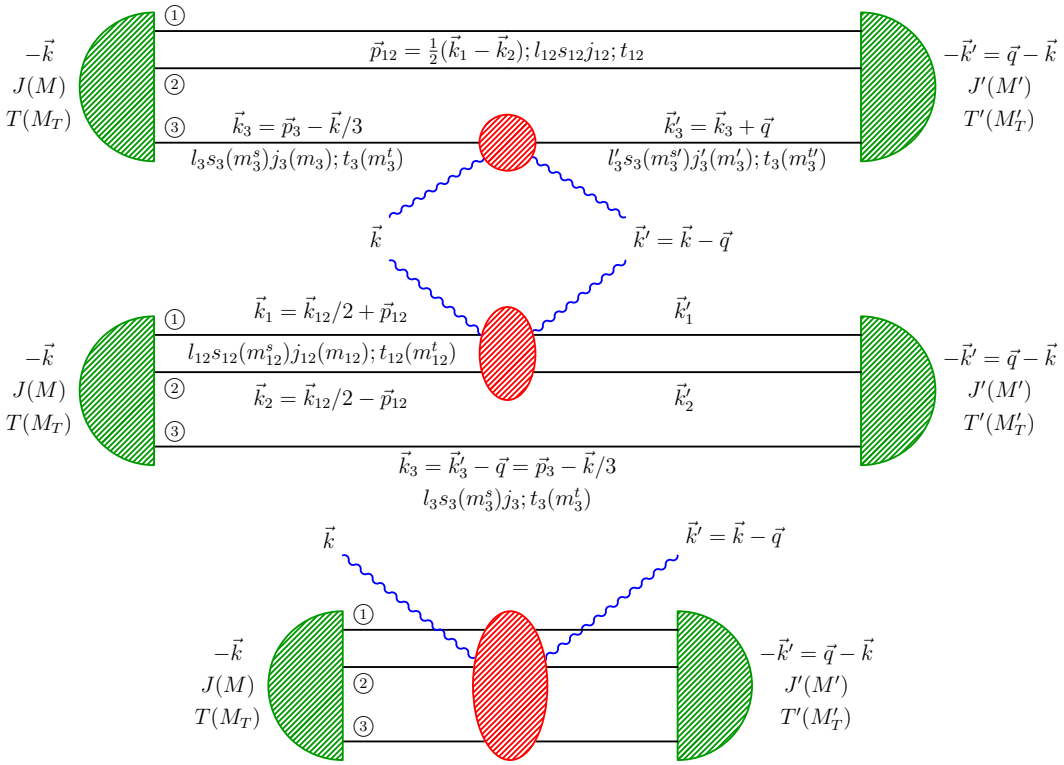

Figure 1: Kinematics in the center of mass frame and quantum numbers for an $A = 3$ system in the case of Compton scattering. Generalization to other reactions only changes the kind of ingoing/outgoing probe. Top: one-body processes $\hat{O}_3$, center: two-body processes$\hat{O}_{12}$, bottom: three-body processes$\hat{O}_{123}$. Green represents the densities, and red represents the kernels. Griesshammer *et al.*[1]

For scattering off an A body nucleus, the total scattering amplitude is given by

$$\begin{aligned} A_M^{M'}(\vec{k},\vec{q}) = &\binom{A}{1}\langle M'|\,\hat{O}_3(\vec{k},\vec{q})\,|M\rangle + \binom{A}{2}\langle M'|\,\hat{O}_{12}(\vec{k},\vec{q})\,|M\rangle \\ &+ \binom{A}{3}\langle M'|\,\hat{O}_{123}(\vec{k},\vec{q})\,|M\rangle + \binom{A}{4}\langle M'|\,\hat{O}_{1234}(\vec{k},\vec{q})\,|M\rangle \\ &+ \ldots + \binom{A}{A}\langle M'|\,\hat{O}_{1\ldots A}(\vec{k},\vec{q})\,|M\rangle\,, \end{aligned} \tag{1}$$

where M, M' is the spin of the target nucleus, and there are $\binom{A}{i}$ ways for a probe to hit i nucleons. Fortunately χEFT provides a hierarchy of scales which predicts decreasing contributions for higher order terms for probe energies greater than ~ 40MeV. To this end we use only the first two terms

$$A_M^{M'}(\vec{k},\vec{q}) = \binom{A}{1}\langle M'|\,\hat{O}_3(\vec{k},\vec{q})\,|M\rangle + \binom{A}{2}\langle M'|\,\hat{O}_{12}(\vec{k},\vec{q})\,|M\rangle$$

In practice this is enough for accuracy on the 5% level.

2. Kernels and Densities

The one-body and two-body kernel need to be considered separately. Their form is completely different, and they require a one and two body density respectively. We now write the wave function in the three body system as the partial-wave decomposition of Jacobi momenta p_i and the relevant quantum numbers α. The wave function in momentum space is given by

$$\psi_\alpha(p_{12},\, p_3) = \langle p_{12} p_3 \alpha | M\rangle\,. \tag{2}$$

The nucleus being described has total angular momentum J and spin-projection M. The momenta are $\vec{p}_{12} = \frac{1}{2}\left(\vec{k}_1 - \vec{k}_2\right)$ where $\vec{p}_3 = \vec{k} + \frac{1}{3}\vec{k}_3$, and $p_{12} = |\vec{p}_{12}|$ and $p_1 = |\vec{p}_1|$. Recall $\vec{k}_i$ are the individual nucleon momenta, and $\vec{k}$ is the probe momentum in the CM frame. The quantity α represents all the quantum numbers of the nucleons inside the nucleus [1]

$$|\alpha\rangle = |[(l_{12}s_{12})\,j_{12}\,(l_3 s_3)\,j_3]\,JM, (t_{12}t_3)\,TM_T\rangle\,, \tag{3}$$

Here s, l and j are the spin, orbital and total angular momentum respectively. The quantum number s_3 simply represent the spin of nucleon 3, whereas s_{12} represents the total spin of the 1-2 subsystem; the quantities l_{12} and j_{12} combine the 1-2 subsystem similarly. Furthermore, s_{12} and l_{12} combine to j_{12} and likewise for l_3, s_3 and j_3. Finally j_{12} and j_3 combine to the total nucleus spin J. The same combinations are done for t_{12}, t_3 and T, with isospin projection M_T. Here t_3 and t_{12} are the isospin of the nucleon labeled 3 and the 1-2 subsystem respectively, T is the isospin of the entire nucleus and M_T is the number of protons minus neutrons over 2. We now seek to describe the scattering amplitudes.

We restrict ourselves to elastic processes, which simplifies the following discussion by requiring that the probe does not change the charge of any of the nucleons. For the one body density, the

one-body kernel of the probe interaction with nucleon 3 is O_3. Leaving nucleons 1 and 2 as spectators [1],

$$\left\langle \vec{k}_3' \left| \left\langle s_3 m_3^{s'} \left| \left\langle t_3 m_3^{t'} \left| \hat{O}_3(\vec{k},\vec{q}) \right| t_3 m_3^{t} \right\rangle \right| s_3 m_3^{s} \right\rangle \right| \vec{k}_3 \right\rangle \\ \equiv \delta_{m_3^{t'} m_3^{t}} \delta^{(3)}\left(\vec{k}_3' - \vec{k}_3 - \vec{q}\right) O_3\left(m_3^{s'} m_3^{s} m_3^{t}; \vec{k}_3; \vec{k}, \vec{q}\right), \tag{4}$$

where m_t and m_t' are the isospin of the active nucleon before and after the interaction (recall $m_t = \pm\frac{1}{2}$ is the proton/neutron). Symbolically, the matrix element $\hat{O}_3$ is:

$$\left\langle M' \left| \hat{O}_3(\vec{k},\vec{q}) \right| M \right\rangle = \sum_{\alpha\alpha'} \int \mathrm{d}p_{12} p_{12}^2 \, \mathrm{d}p_3 p_3^2 \, \mathrm{d}p_{12}' p_{12}'^2 \, \mathrm{d}p_3' p_3'^2 \psi^\dagger_{\alpha'}\left(p_{12}' p_3'\right) \psi_\alpha\left(p_{12} p_3\right) \\ \times \left\langle p_{12}' p_3' \left[\left(l_{12}' s_{12}'\right) j_{12}' \left(l_3' s_3\right) j_3' \right] J' M' \left(t_{12}' t_3\right) T' M_T \right| \hat{O}_3(\vec{k},\vec{q}) \\ \left| p_{12} p_3 \left[\left(l_{12} s_{12}\right) j_{12} \left(l_3 s_3\right) j_3 \right] J M \left(t_{12} t_3\right) T M_T \right\rangle . \tag{5}$$

The central result is that up to relativistic corrections, this can be written as:

$$\left\langle M' \left| \hat{O}_3(\vec{k},\vec{q}) \right| M \right\rangle = \sum_{\substack{m_3^{s'} m_3^{s} \\ m_3^{t}}} \hat{O}_3\left(m_3^{s'} m_3^{s}, m_3^{t}; \vec{k}, \vec{q}\right) \rho^{m_3^t M_T, M'M}_{m_3^{s'} m_3^{s}}(\vec{k},\vec{q}) \, . \tag{6}$$

Here ρ, is the *one-body transition density amplitude* for the nucleus which was discussed previously and can truly be interpreted as the probability amplitude that nucleon m_3^t absorbs momentum $\vec{q}$, changes its spin projection from m_s^3 to $m_s^{3'}$ and changes the spin-projection of the nucleus from M to M'. Its operator form is

$$\rho^{m_3^t M_T, M'M}_{m_3' m_3^s}(\vec{k},\vec{q}) = \left\langle M' \left| s_3 m_3^{s'}, t_3 m_3^t \right\rangle \mathrm{e}^{\mathrm{i}\frac{2}{3}\vec{q}\cdot\vec{r}_3} \left\langle s_3 m_3^s, t_3 m_3^t \right| M \right\rangle . \tag{7}$$

The two body case works similarly, and results in

$$\left\langle M' \left| \hat{O}_{12} \right| M \right\rangle = \sum_{\alpha_{11}', \alpha_{12}} \int \mathrm{d}p_{12} \, p_{12}^2 \, \mathrm{d}p_{12}' \, p_{12}'^2 \, O_{12}^{\alpha_{12}' \alpha_{12}}\left(p_{12}', p_{12}\right) \rho^{M_T, M'M}_{\alpha_{12}' \alpha_{12}}\left(p_{12}', p_{12}; \vec{q}\right) \, . \tag{8}$$

This is the two-body equivalent to (6). There is an expression analogous to (5) but, it is non-trivial and for our purposes non-enlightening. This two-body density $\rho^{M_T, M'M}_{\alpha_{12}' \alpha_{12}}$ is of course completely distinct from the one-body density. However, just like the one-body case it can also be interpreted as a probability density. It is dependent on the incoming and outgoing quantum numbers α_{12} and α_{12}' of the 1-2 system, and also on the relative momenta of the two nucleons which are integrated over. As a result, the total file size for the two nucleon densities are on the order of a few GB per energy and angle, whereas those of the one nucleon densities are on the order of a few KB. Importantly, ρ can be computed generically from a nuclear potential, such as the chiral SMS potential without reference to the kernel $\hat{O}_3$ or $\hat{O}_{12}$ [2]. *Maybe this is too much detail.*

3. SRG Transform

Previous work using the transition density method has looked at ^{3}He and ^{4}He but to extend this ^{6}Li ($A = 6$) involves many body interactions which are much more complicated, and numerically

expensive [1, 3]. To this end a similarity renormalization group (SRG) transformation is used [4]. When using nuclear potentials, we approximate the potential to be zero outside of a certain cutoff Λ, and therefore neglect it in our calculation. In general a nuclear potential, such as the chiral SMS potential does not fall off quickly for high momenta meaning we would have to extend the cutoff much further than we would like which in turn increases computation cost. The SRG transform is a unitary transformation that allows us to shovel all the dependence into the low momentum region making calculation for $A = 6$ possible. The SRG transformation can be thought of as a local averaging or smoothing out of the potential, resulting in decreased "resolution" has the SRG is applied. In the unevolved, high resolution figure 2a one can see the potential does not go to zero

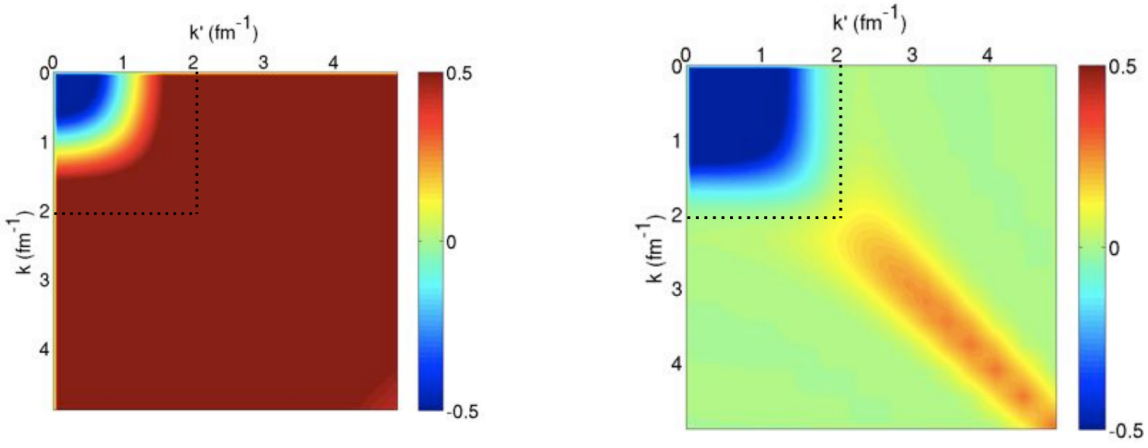

(a) High Resolution (bare, unevolved potential)

(b) Low Resolution (evolved)

Figure 2: Nuclear potentials $V(k, k')$. Figures from Kai Hebeler: "Chiral Effective Field Theory and Nuclear Forces: overview and applications" presentation at TALENT school at MITP 2022

quickly whereas once the transformation is applied in figure 2b it does. As a result a cutoff can be made at $k, k' = 2\text{fm}^{-1}$ without losing much accuracy. In the example above, if the unevolved potential had to be consider up to $k, k' = 5$, this means an efficiency gain proportional to the areas of each, for a factor of $(5/2)^2 = 6.25$.

However, this creates another problem; the SRG transform creates a change in physical meaning of the momenta free variables. To understand this, let us first consider an example the reader is certainly more familiar with - a Fourier transformation which changes a potential from position to momentum space.

$$V(\vec{r}, \vec{r}\,') = \langle r' | \, V \, | r \rangle = \int \mathrm{d}^3 p \, \mathrm{d}^3 p' \, \langle r' | p' \rangle \, \langle p' | \, V \, | p \rangle \, \langle p | r \rangle \, = V(\vec{p}, \vec{p}\,') \tag{9}$$

After the transform our free variables have different physical meaning. In fact, any unitary transform,

also transforms the coordinates.

$$\begin{aligned}\langle p'|\,V\,|p\rangle &= \langle p'|\,\mathbb{1}V\mathbb{1}\,|p\rangle \\ &= \langle p'|\,U^\dagger UVU^\dagger U\,|p\rangle \\ &= \left(\langle p'|\,U^\dagger\right)\,\left(UVU^\dagger\right)\,\left(U\,|p\rangle\right) \\ &= \langle \widetilde{p}\,'|\,V_{eff}\,|\widetilde{p}\rangle = V_{eff}(\widetilde{p},\widetilde{p}\,')\end{aligned} \tag{10}$$

So calling the free variables in an SRG transformed potential "momenta" is abuse of notation. They are not physical states in the sense that $\widetilde{p} = 50$MeV does not correspond to a state of 50 MeV an experimentalist can prepare. The Lagrangians that generate the Feynman diagrams in the kernel however have dependence on physical momenta and therefore we cannot directly use an SRG evolved potential in the non-SRG evolved kernel. To solve this, previous work with SRG transformations has transformed the Lagrangians into the SRG evolved space, however in the case of the density formalism this would mean adding SRG information into the kernel, thereby breaking kernel-density independence. Additionally, the SRG transformation can take many different forms; the state of the art transformation has changed over the years, and we wish to allow for these developments without having to re-write the kernel code. Therefore Xiang-Xiang Sun *et al.*have chosen to apply an inverse transformation to the densities. This work was begun with the highest nucleon number system we can calculate densities for without an SRG transformation, which is ^{4}He. In this way we have gained confidence in ^{4}He before moving to the more complex ^{6}Li. *Are they not publishing a paper on this? How do I credit Xiang-Xiang effectively?* In figure 3 we see the effectiveness of the

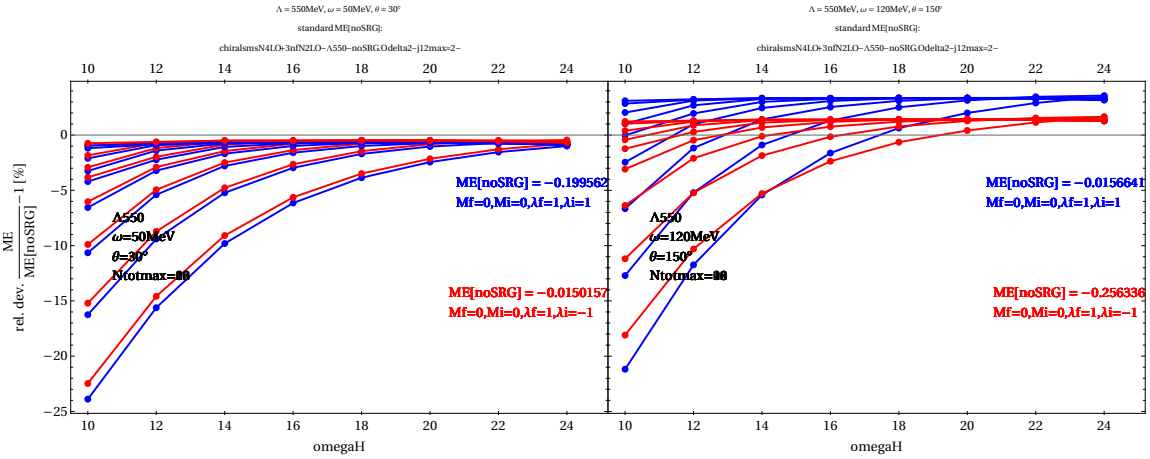

Figure 3: A convergence plot for ^{4}He Compton scattering showing the relative deviation of the matrix elements (ME) of the reaction.

results in the ^{4}He case. The SRG transformation uses the harmonic oscillator basis, and the value 'omegaH' on the x-axis is the width of the harmonic oscillator potential, and 'Ntotmax' is the total number of states used. With this completed we have now moved to ^{6}Li. This is of much interest experimentally since this target is stable solid at room temperature, it is therefore easy to conduct an experiment on, even to high precision due to its relatively large cross section. ^{6}Li *results go here. We have many more results since the actual chiral dynamics presentation - they go here.*

4. Analyzing Different Interactions

4.1 Compton Scattering

Compton scattering allows for extraction of the nucleon polarizabilites. α_{E1}, β_{M1}, a subject of much experimental interest. These parameters quantify the stiffness of a nucleus, and enter in the Hamiltonian via

$$\mathcal{H} = -4\pi \left(\frac{1}{2}\alpha_{E1}\vec{E}^2 + \frac{1}{2}\beta_{M1}\vec{H}^2 \right) \tag{11}$$

There are many experiments on ^{6}Li, yet as of now there is no theory prediction [10, 11]. We seek to fill this gap.

Beyond Compton scattering we are interested in extending the density formalism to other processes. In particular pion-photoproduction, and pion-pion scattering are of interest. Fortunately their kernels share remarkable similarity since there are only so many ways for one particle to go in and one to go out. *I don't want to include that diagram since I stole the figures from somewhere, but I don't remember where*

4.2 Pion-Photoproduction

For the pion-photoproduction one-body kernel we use the results of scattering on a single nucleon, $\gamma N \rightarrow \pi N$ which has been studied extensively. Its differential cross section can be decomposed in terms of the electric and magnetic multipoles $E_{l\pm}, M_{l\pm}$ which are angle independent [5]. There have been many experimental results over the years which measure these multipoles to high order and with good precision such as "Unified Chew-Mandelstam SAID analysis..." Workman *et al.*[6]. The scattering matrices $\mathcal{M}$ which result from this are exactly what enters as $\hat{O}_3$ in equation (6). This solves a significant problem since calculation of the one-body pion-photoproduction kernel to high accuracy directly through Feynman diagrams requires including many terms in the chiral expansion due to the proximity of the $\Delta(1232)$ resonance at $\sim$ 200MeV [7].

The two-body contributions do not easily decompose into multipole interactions, therefore we preform the calculation through expansions in the chiral Lagrangian through calculation of Feynman diagrams. At threshold energy this reaction kernel has been analyzed by Lenkewitz *et al.*[8, 9]. We now have a numerically stable result for ^{3}He and seek to extend this to new targets.

4.3 Pion-Pion scattering and other reactions

The pion-pion scattering kernel is similar to the pion photoproduction kernel. Beane *et al.*has developed this kernel at threshold for both one-body and two-body interactions [12]. We may extend this to finite energy. When the pion-photoproduction and pion-pion scattering kernels have successfully been developed, we will instantly be able to calculate all of these reactions on targets previously analyzed in the density formalism since we already have produced the densities required. In particular, we will calculate all of these reactions with the targets ^{3}He, ^{4}He, and ^{6}Li.

5. Conclusion

References

[1] H. W. Grießhammer, J. A. McGovern, A. Nogga, and D. R. Phillips, "Scattering Observables from One- and Two-body Densities: Formalism and Application to γ^3 Scattering," *Few-Body Systems*, vol. 61, no. 4, Nov. 2020. DOI: 10.1007/s00601-020-01578-w.

[2] P. Reinert, H. Krebs, and E. Epelbaum, "Semilocal momentum-space regularized chiral two-nucleon potentials up to fifth order," *The European Physical Journal A*, vol. 54, no. 5, May 2018. DOI: 10.1140/epja/i2018-12516-4.

[3] H. W. Griesshammer, J. Liao, J. A. McGovern, A. Nogga, and D. R. Phillips, "Compton Scattering on 4He with Nuclear One- and Two-Body Densities," arXiv:2401.16995.

[4] S. Szpigel and R. J. Perry, "The Similarity Renormalization Group,". arXiv:hep-ph/0009071.

[5] R. L. Walker, "Phenomenological Analysis of Single-Pion Photoproduction," *Phys. Rev.*, vol. 182, no. 5, pp. 1729–1748, Jun. 1969. DOI: 10.1103/PhysRev.182.1729.

[6] R. L. Workman, M. W. Paris, W. J. Briscoe, and I. I. Strakovsky, "Unified Chew-Mandelstam SAID analysis of pion photoproduction data," *Phys. Rev. C*, vol. 86, no. 1, p. 015202, Jul. 2012. DOI: 10.1103/PhysRevC.86.015202.

[7] N. Rijneveen, A. M. Gasparyan, H. Krebs, and E. Epelbaum, "Pion photoproduction in chiral perturbation theory with explicit treatment of the $\Delta(1232)$ resonance," arXiv:2108.01619.

[8] M. Lenkewitz, E. Epelbaum, H.-W. Hammer, and U.-G. Meißner, "Neutral pion photoproduction off ^{3}H and ^{3}He in chiral perturbation theory," *Physics Letters B*, vol. 700, no. 5, pp. 365–368, Jun. 2011. DOI: 10.1016/j.physletb.2011.05.036.

[9] M. Lenkewitz, E. Epelbaum, H.-W. Hammer, and U.-G. Meissner, "Threshold neutral pion photoproduction off the tri-nucleon to $O(q^4)$," *The European Physical Journal A*, vol. 49, no. 2, Feb. 2013. DOI: 10.1140/epja/i2013-13020-1.

[10] L. S. Myers, M. W. Ahmed, G. Feldman, A. Kafkarkou, D. P. Kendellen, I. Mazumdar, J. M. Mueller, M. H. Sikora, H. R. Weller, and W. R. Zimmerman, "Compton scattering from ^{6}Li at 86 MeV," *Phys. Rev. C*, vol. 90, no. 2, p. 027603, Aug. 2014. DOI: 10.1103/PhysRevC.90.027603.

[11] L. S. Myers, M. W. Ahmed, G. Feldman, S. S. Henshaw, M. A. Kovash, J. M. Mueller, and H. R. Weller, "Compton scattering from ^{6}Li at 60 MeV," *Phys. Rev. C*, vol. 86, no. 4, p. 044614, Oct. 2012. DOI: 10.1103/PhysRevC.86.044614.

[12] S. R. Beane, V. Bernard, E. Epelbaum, U.-G. Meißner, and D. R. Phillips, "The S-wave pion–nucleon scattering lengths from pionic atoms using effective field theory," *Nuclear Physics A*, vol. 720, no. 3–4, pp. 399–415, Jun. 2003. DOI: 10.1016/S0375-9474(03)01008-X.